LETTERS

Spatial vegetation patterns and imminent desertification in Mediterranean arid ecosystems

Sonia Kéfi[1], Max Rietkerk[1], Concepción L. Alados[2], Yolanda Pueyo[1], Vasilios P. Papanastasis[3], Ahmed ElAich[4] & Peter C. de Ruiter[1,5]

Humans and climate affect ecosystems and their services[1], which may involve continuous and discontinuous transitions from one stable state to another[2]. Discontinuous transitions are abrupt, irreversible and among the most catastrophic changes of ecosystems identified[1]. For terrestrial ecosystems, it has been hypothesized that vegetation patchiness could be used as a signature of imminent transitions[3,4]. Here, we analyse how vegetation patchiness changes in arid ecosystems with different grazing pressures, using both field data and a modelling approach. In the modelling approach, we extrapolated our analysis to even higher grazing pressures to investigate the vegetation patchiness when desertification is imminent. In three arid Mediterranean ecosystems in Spain, Greece and Morocco, we found that the patch-size distribution of the vegetation follows a power law. Using a stochastic cellular automaton model, we show that local positive interactions among plants can explain such power-law distributions. Furthermore, with increasing grazing pressure, the field data revealed consistent deviations from power laws. Increased grazing pressure leads to similar deviations in the model. When grazing was further increased in the model, we found that these deviations always and only occurred close to transition to desert, independent of the type of transition, and regardless of the vegetation cover. Therefore, we propose that patch-size distributions may be a warning signal for the onset of desertification.

It is of the utmost importance to find early warning signals of transitions that can alter ecosystems' services in fundamental ways, causing losses of ecological and economic resources[2,4]. Determining proximity to transitions is especially important for arid ecosystems, which may convert into deserts[2,4,5]. According to the Millennium Ecosystem Assessment, increasing external pressures by human activities or climate change will lead to desertification, affecting the livelihood of more than 25% of the world's population[1]. A mechanism playing a dominant role in the functioning of arid ecosystems is local facilitation among plants[6–9]. Local facilitation is the biophysical ameliorative effect of sessile organisms, such as plants, on their neighbouring environment. Such local positive interactions induce vegetation patchiness[6,7,10] and determine the response of this patchiness to environmental change[3].

We investigated how the spatial organization of vegetation is influenced by the degree of external stress by combining modelling and field data from three grazed Mediterranean arid ecosystems in Spain, Greece and Morocco. In each of these ecosystems, we collected data on three sites that differed with respect to the livestock grazing pressure (Table 1; Methods). In each of the nine (3×3) sites, we analysed the number and the sizes of the vegetation patches (see Methods), and plotted the number of patches, $N(S)$, as a function of their sizes, S. We fitted these patch-size distributions to two different models: a power law, $N(S) = CS^{-\gamma}$; and a truncated power law, $N(S) = CS^{-\gamma}e^{-\frac{S}{S_x}}$, where γ is the estimated scaling exponent of the model, S_x the patch size (in centimetres) above which $N(S)$ decreases faster than in a power law, and C is a constant[11,12]. To understand the mechanisms that may be responsible for the spatial organization of the vegetation, the observed distributions were compared with distributions generated by a stochastic cellular automaton model (see Methods).

We focused first on the spatial organization of the field sites with the lowest grazing pressure. In the three ecosystems, a power law best fitted the patch-size distribution characterized by a linear relation on a logarithmic scale (Fig. 1a, d and g). This power-law relation implied that vegetation patches were present over a wide range of size scales, with many small patches and relatively few large ones. The values of the scaling exponents γ of these power laws are similar among the three ecosystems, which is consistent with the hypothesis of a universal mechanism of Mediterranean ecosystem organization. At the

Table 1 | Characteristics of the three Mediterranean ecosystems

	Ecosystem type*	Dominant species	Climate	Effective stocking rate (animals per hectare per year)	Transect size (m)
Cabo de Gata-Nijar Natural Park (Almeria province, Spain)	Scattered matorral (scrubland)	*Stipa tenacissima, Chamaerops humilis, Periploca laevigata, Thymus hyemalis, Brachypodium retusum*	Average rainfall, 200 mm; mean annual temperature, 18 °C; altitude, 100 m; AI = 9.0†	Low, 0; middle, 0.27; high, 0.46	32 m (30 transects per field site)
Uta (Sithonia peninsula, Greece)	Dense matorral (shrubland)	*Cistus monspeliensis, Phillyrea latifolia, Pistacia lentiscus*	Average rainfall, 590 mm; mean annual temperature, 16.2 °C; altitude, 50 m; AI = 2.75†	Low, 0.3; middle, 2.6; high, 8.2	32 m (30 transects per field site)
Timahdit (Middle Atlas mountains, Morocco)	High mountain grassland	*Carex divisa, Genista pseudopilosa, Poa bulbosa, Thymus hyemalis*	Average rainfall, 800 mm; mean annual temperature, 22 °C; altitude, 1,900 m; AI = 2.75†	Low, 0.9; middle, 1.54; high, 2.49	16 m (30 transects per field site)

* See ref. 28 for more details.
† The aridity index[29] AI is defined as $AI = 100T/P$, where T is the average annual temperature in °C and P is the average annual rainfall in mm. AI = 2–3 characterizes a semi-arid area. AI > 3 characterizes an arid area.

[1]Department of Environmental Sciences, Copernicus Institute, Utrecht University, PO Box 80115, 3508 TC Utrecht, The Netherlands. [2]Pyrenean Institute of Ecology, Avda. Montañana 1005. Apdo. 202, 50192 Zaragoza, Spain. [3]Laboratory of Rangeland Ecology, Aristotle University, 54006 Thessaloniki, Greece. [4]Département des Productions Animales, Institut Agronomique et Vétérinaire Hassan II, Rabat, Morocco. [5]Soil Center, Wageningen University and Research Center, Droevendaalsesteeg 4, 6708 PB Wageningen, The Netherlands.

sites with higher grazing pressure, we found that a truncated power law best described the patch-size distribution: that is, there was a consistent deviation from a power law for all three ecosystems (Fig. 1b, c, e, f, h and i). The scaling exponents γ of these truncated power laws have smaller values than the γ estimated for the power-law relations. These deviations from power laws are due to a deficiency of large patches in areas described by truncated power laws compared to power laws.

To identify the mechanisms responsible for generating the power laws and their deviations, we constructed a spatial model (see Methods) of arid ecosystems. The model described arid ecosystems as lattice-structured habitats, in which each cell is occupied by vegetation (denoted +), unoccupied by vegetation (denoted 0), or degraded (denoted −). At each time step, the status of each cell can change with a probability per unit of time, depending on the status of the cell and its neighbours. Plants reproduce by spreading seeds throughout the lattice. A fraction of the seeds is dispersed locally, whereas the rest is dispersed globally[13]. The recruitment of a new individual has a probability of being successful only if the seeds reach a {0}-cell and depends on global competition for resources (negative density-dependence). The mortality of a {+}-cell occurs at a density-independent rate and may turn a {+}-cell into a {0}-cell. A {0}-cell may undergo further degradation, for example, by processes such as erosion and soil crust formation. This may turn a {0}-cell into a {−}-cell in a density-independent manner. Regeneration of a {−}-cell is faster when there are more {+}-cells in its neighbourhood, because of the positive effect of vegetation on its micro-environment; this is how local facilitation is modelled. We call a system with no vegetation cells a desert. Local positive interactions include local facilitation and local seed dispersal. We model grazing pressure as higher mortality of {+}-cells, which is the minimal possible way of including grazing in our model[14]. Grazing may include other effects, such as soil trampling or non-random movement of the animals that we do not take into account in our model. We present the model results for varying grazing pressure, but varying aridity has the same qualitative effect.

The model results showed that in systems with low grazing pressure strong local positive interactions (that is, strong local facilitation and a large proportion of seeds locally dispersed) led to a patch-size distribution characterized by a power law (Fig. 2a). When we decreased the strength of local positive interactions, the patch-size distribution deviated from a power law (Fig. 2b, c). In other words, strong local positive interactions are needed in our model to produce a power-law distribution at low grazing pressure. Without local positive interactions, power laws are never observed in our model. Thus, local positive interactions can explain the spatial organization of vegetation in the form of power laws in the three arid Mediterranean ecosystems with the lowest grazing pressure. We do not intend to prove here that local facilitation is the only possible mechanism generating the observed power laws. However, local facilitation is generally recognized as a dominant ecological mechanism driving the dynamics of arid ecosystems, and is more specifically known to operate in the three ecosystems where we collected the data[7,10]. So, our model results suggest that local facilitation is (at least) one of the mechanisms at the origin of the observed power laws.

When we increased grazing pressure in our model, while keeping the local positive interactions strong, the patch-size distribution deviated from a power law in a way similar to what was observed (Fig. 2d–f). In the model, the effect of increasing grazing pressure appeared to be similar to the effect of decreasing the strength of local positive interactions (Fig. 2). This can be understood intuitively

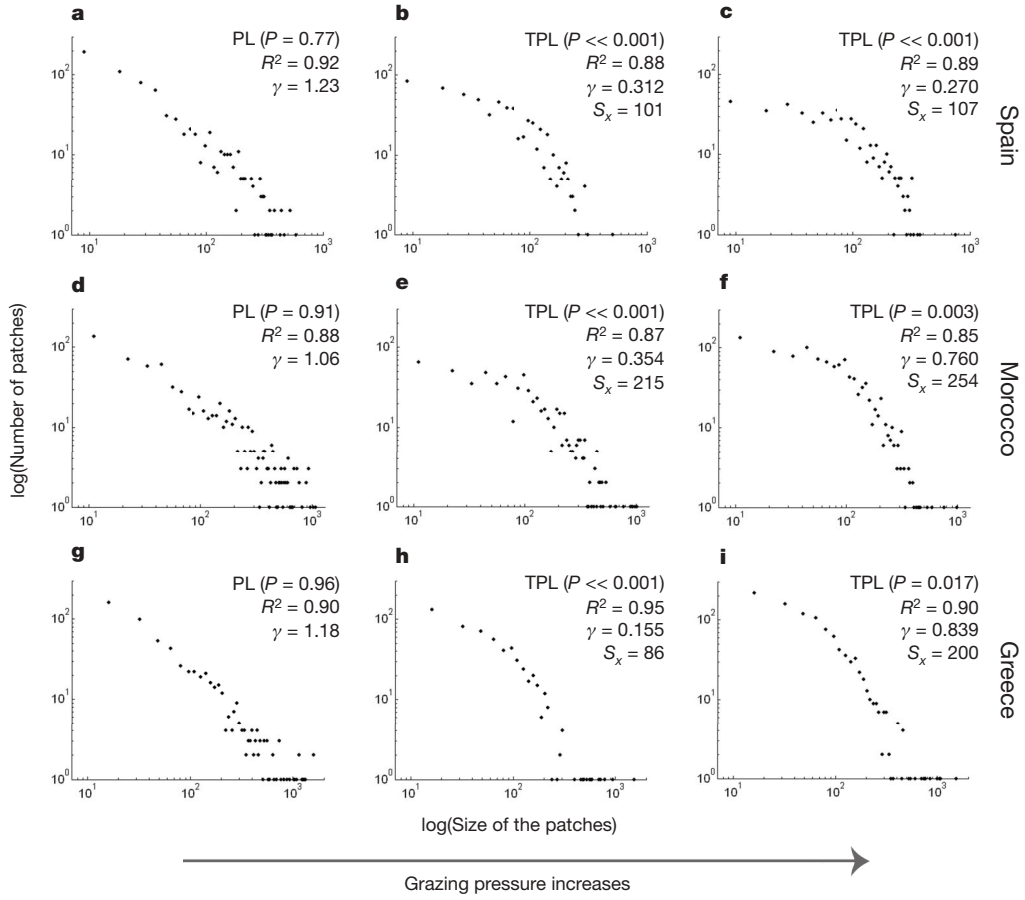

Figure 1 | Effect of grazing on the patch-size distribution of vegetation in three Mediterranean ecosystems. Increasing grazing intensity from left to right (see Table 1 for the grazing intensities). **a–c**, Spain. **d–f**, Greece. **g–i**, Morocco. The *P*-value of the sum of square reduction test, the R^2 of the best-fitted model (either power law, PL, or truncated power law, TPL), γ and S_x (see text) are given.

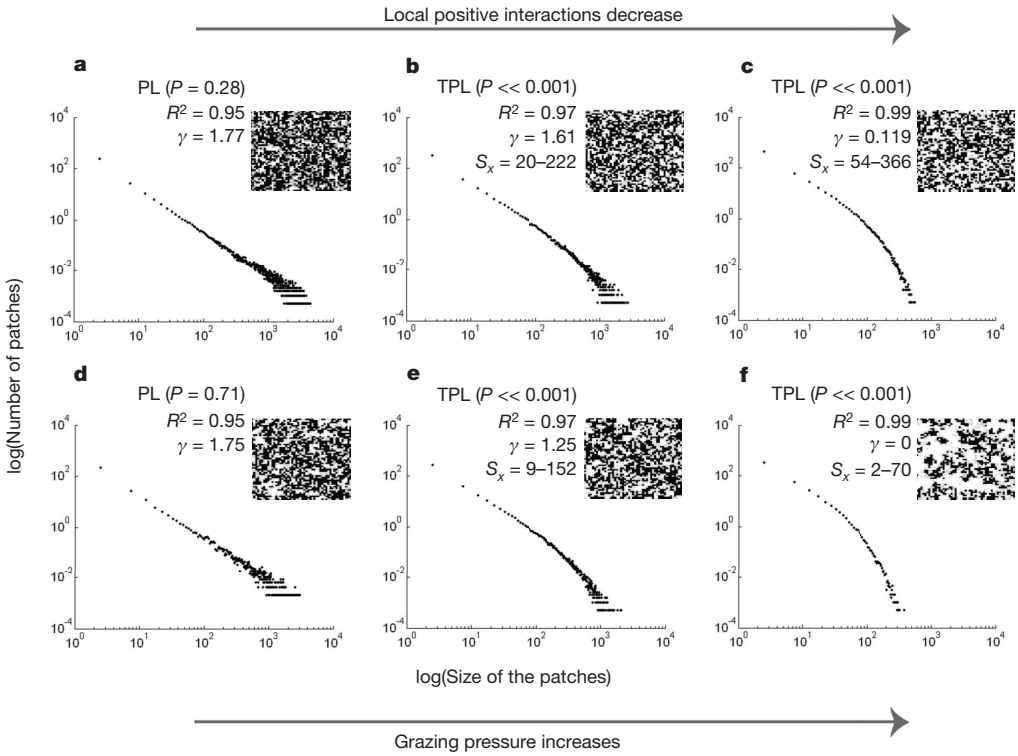

Figure 2 | Effect of local positive interactions and grazing pressure on the patch-size distribution in the model. **a–c**, Decreasing local positive interactions from left to right. **d–f**, Increasing grazing pressure from left to right. P, R^2, γ and S_x are given (see legend to Fig. 1). The first value given for S_x is a number of grid cells. Taking the square root of this value, and considering 50 cm as the length of a grid cell, leads to the second value, in centimetres. Insets are snapshots of the system at the end of the simulation. Black, vegetation; grey, recolonizable; white, degraded. See Methods for the parameter values.

because local positive interactions are crucial in maintaining vegetation in the model system, and even more so when the level of grazing pressure is high. If grazing pressure increases, stronger local positive interactions are required to maintain the system in a similar vegetation state. If the strength of local positive interactions remains the same (no plant adaptation), there is a level of grazing at which local positive interactions cannot prevent the vegetation from extinction. Thus, our model results are in agreement with our observations from Mediterranean arid ecosystems that increased grazing pressure leads to patch-size distributions that deviate from power laws, because of a decrease in the frequency of large patches.

The scaling exponents γ of the power laws obtained in the model are similar to the values observed in the data, although slightly higher (compare Fig. 2a, d with Fig. 1a, d and g). Consistent with the data, the scaling exponent γ estimated for the truncated power law is always smaller than the one estimated for the power law (Fig. 2b, c, e and f). The S_x values are of the same order of magnitude as the values estimated for the field data.

The model simulation results also showed that transitions from a vegetated to a desert state could be continuous or discontinuous (Fig. 3). At low grazing pressure, the density of vegetation gradually decreases towards zero with increasing aridity (Fig. 3a). The transition is then called continuous. However, if the grazing pressure is high, the density of vegetation undergoes discontinuous transitions with increasing aridity (Fig. 3b). This is because the system becomes bistable close to transition (Fig. 3b). Indeed, when mortality is higher

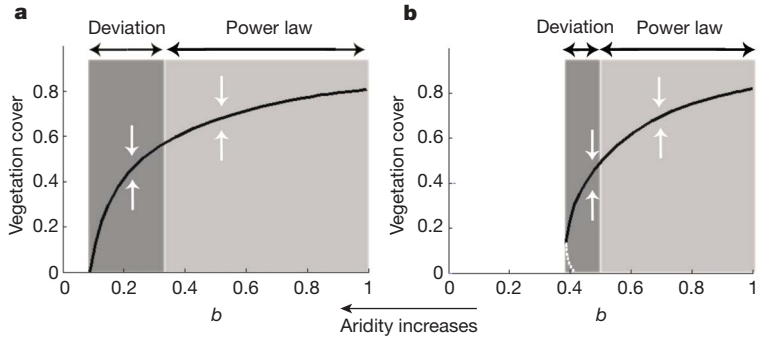

Figure 3 | Localization of the deviation to a power law along transitions in the model. Bifurcation diagrams numerically obtained from a correlation approximation of the model (Methods; see ref. 3). **a**, Continuous transition, low grazing. **b**, Discontinuous transition, high grazing. Vertical axis: fraction of the lattice occupied by vegetation at equilibrium. Horizontal axis: a lower b value reflects higher aridity. Black line, stable equilibria. Grey dashed line, unstable equilibria. Dark grey areas, deviation from power law. Light grey areas, power law. The limit value of b between the dark grey and the light grey areas was determined numerically by running the model for different b values, and by then testing which was the best-fitted model (**a**, $b = 0.34 \pm 0.01$; **b**, $b = 0.50 \pm 0.01$). White arrows indicate the direction of change of the system if the equilibrium is perturbed. See Methods for the parameter values.

because of grazing, vegetation cells might not have time to form viable patches before they die. Whether vegetation can survive in the system may then depend on the initial vegetation density, leading to bistability. In this case, a decrease in aridity to the values for which the transition occurred does not necessarily lead to a recovery of the vegetation (hysteresis). Both along continuous and discontinuous transitions, our model simulations showed that the patch-size distribution deviates from a power law just before the transition point to a desert (Fig. 3). Thus, these deviations from a power law are a general behaviour of the model system close to transition, independent of the type of transition (Fig. 3), and regardless of the vegetation cover (Fig. 2c, f).

As far as we know, power laws have not previously been described for patch-size distribution of vegetation in arid ecosystems. Power laws are commonly found in a number of biological systems[12,15–19] and physical systems (for example, see ref. 20), but the mechanisms generating them are not clearly understood in the case of ecosystems. Our study showed that local positive interactions can be responsible for power-law distributions of vegetation patches in arid Mediterranean ecosystems with a low grazing pressure. Deviations from power laws because of a deficiency of large patches in systems with high grazing pressure always occur closer to transitions than do the power laws themselves. Our model behaves differently from classical critical systems[21], where power laws only occur at the transition point. This may be explained by a major mechanistic difference between our model and classical critical models that we now address.

In classical critical systems, such as wind-disturbed tropical forests or wave-disturbed intertidal mussel beds, the abiotic disturbance (for example, wind or waves) removes the susceptible cells (occupied by trees or mussels) from the system, thereby creating disturbed cells (empty cells that are recolonizable). The intensity of the abiotic disturbance increases with the local density of disturbed cells, leading to 'active' propagation of the disturbance[22]. In those systems, the spread of the disturbance shapes the patch-size distribution. Therefore it makes sense that power laws occur for strong disturbances, corresponding to systems close to extinction. In our system, the vegetation spread (rather than the propagation of the disturbance) determines the patch-size distribution. In our system, the disturbance is a degradation process that only affects recolonizable cells creating degraded cells; so the disturbance does not directly affect the susceptible cells (in our model, the vegetation cells). The existence of a third status, recolonizable, as a necessary stage between susceptible and disturbed constrains the spatial propagation of the disturbance. We thus expect power laws to occur for high vegetation densities, corresponding to systems far from extinction.

Arid ecosystems are among the most sensitive ecosystems to global climate change[23]. High grazing pressure pushes arid ecosystems towards the edge of extinction[1]. Increased aridity can then lead to desertification in a discontinuous way, where the possibility of recovery will be low[2–4,14]. How the consistent deviations from power laws exactly relate to desertification in the field is an important and urgent question for future research, because our model results suggest that such deviations may be early warning signals for desertification of arid ecosystems.

METHODS SUMMARY

In the nine field sites, effective stocking rates (animals per hectare per year) were calculated by observation of animals. Vegetation surveys were performed on 30 random transects per site using the line-intercept method. We define a 'patch' as a distance on a transect that is totally covered by vegetation. For each site we examined the non-cumulative patch-size distribution: that is, the relationship between patch number and patch size. The two possible (nested) models for the patch-size distribution on a logarithmic scale—power law or truncated power law—were compared with a sum of square reduction test at a 5% significance level[24].

The model simulations (see Methods for model details) were carried out on grids of 100×100 cells by using a stochastic asynchronous update algorithm of the cellular automaton[25]. Two {+}-cells are part of the same patch if they have one of their four edges in common, which is consistent with the data analysis. To derive the non-cumulative patch-size distribution, we used size-classes of five cells, and evaluated the number of patches in each class. The comparison between the two models for the patch-size distributions on a logarithmic scale was done in the same way as for the data. The aridity level was estimated by b, the probability of recruitment of a new vegetation cell in a system without competition. We used the correlation approximation[26] to get numerically derived bifurcation diagrams, using the CONTENT software[3,27]. Along the transitions, we numerically determined the value of the bifurcation parameter at which the best-fitted model switches from power law to truncated power law. We did that by running the model for different aridity levels, plotting the patch-size distribution, and testing which of the two models best fits statistically.

Full Methods and any associated references are available in the online version of the paper at www.nature.com/nature.

Received 27 June; accepted 24 July 2007.

1. Millennium Ecosystem Assessment. *Ecosystems and Human Well-Being: Desertification Synthesis* (World Resources Institute, Washington DC, 2005).
2. Scheffer, M., Carpenter, S., Foley, J. A., Folke, C. & Walker, B. Catastrophic shifts in ecosystems. *Nature* **413,** 591–596 (2001).
3. Kéfi, S., Rietkerk, M., van Baalen, M. & Loreau, M. Local facilitation, bistability and transitions in arid ecosystems. *Theor. Popul. Biol.* **71,** 367–379 (2007).
4. Rietkerk, M., Dekker, S. C., de Ruiter, P. C. & van de Koppel, J. Self-organized patchiness and catastrophic shifts in ecosystems. *Science* **305,** 1926–1929 (2004).
5. Reynolds, J. F. *et al.* Global desertification: Building a science for dryland development. *Science* **316,** 847–851 (2007).
6. Aguiar, M. R. & Sala, O. E. Patch structure, dynamics and implications for the functioning of arid ecosystems. *Trends Ecol. Evol.* **14,** 273–277 (1999).
7. Alados, C. L. *et al.* Association between competition and facilitation processes and vegetation spatial patterns in alpha steppes. *Biol. J. Linn. Soc.* **87,** 103–113 (2006).
8. Callaway, R. M. & Walker, L. R. Competition and facilitation: a synthetic approach to interactions in plant communities. *Ecology* **78,** 1958–1965 (1997).
9. Schlesinger, W. H. *et al.* Biological feedbacks in global desertification. *Science* **247,** 1043–1048 (1990).
10. Pugnaire, F. I., Haase, P. & Puigdefabregas, J. Facilitation between higher plant species in a semiarid environment. *Ecology* **77,** 1420–1426 (1996).
11. Jordano, P., Bascompte, J. & Olesen, J. M. Invariant properties in coevolutionary networks of plant–animal interactions. *Ecol. Lett.* **6,** 69–81 (2003).
12. Solé, R. V. & Bascompte, J. in *Self-organization in Complex Ecosystems* Ch. 6, 215–262 (Princeton Univ. Press, Princeton, 2006).
13. Iwasa, Y. in *The Geometry of Ecological Interactions. Simplify Ecological Complexity* (eds Dieckmann, U., Law, R. & Metz, J. A. J.) 227–251 (Cambridge Univ. Press, Cambridge, 2000).
14. Noy-Meir, I. Stability of grazing systems: an application of predator–prey graphs. *J. Ecol.* **63,** 459–481 (1975).
15. Brown, J. H. *et al.* The fractal nature of nature: power laws, ecological complexity and biodiversity. *Phil. Trans. R. Soc. Lond. B* **357,** 619–626 (2002).
16. Guichard, F., Halpin, P. M., Allison, G. W., Lubchenco, J. & Menge, B. A. Mussel disturbance dynamics: signatures of oceanographic forcing from local interactions. *Am. Nat.* **161,** 889–904 (2003).
17. Malamud, B. D., Morein, G. & Turcotte, D. L. Forest fires: an example of self-organized critical behavior. *Science* **281,** 1840–1842 (1998).
18. Vandermeer, J. & Perfecto, I. A keystone mutualism drives pattern in a power function. *Science* **311,** 1000–1002 (2006).
19. Venegas, J. G. *et al.* Self-organized patchiness in asthma as a prelude to catastrophic shifts. *Nature* **434,** 777–782 (2005).
20. Bak, P., Tang, C. & Wiesenfeld, K. Self-organized criticality. *Phys. Rev. A.* **38,** 364–374 (1988).
21. Sornette, D. *Critical Phenomena in Natural Sciences: Chaos, Fractals, Selforganization and Disorder: Concepts and Tools* (Springer, Berlin/Heidelberg, 2004).
22. Pascual, M. & Guichard, F. Criticality and disturbance in spatial ecological systems. *Trends Ecol. Evol.* **20,** 88–95 (2005).
23. Schröter, D. *et al.* Ecosystem service supply and vulnerability to global change in Europe. *Science* **310,** 1333–1337 (2005).
24. Schabenberger, O. & Pierce, F. J. *Contemporary Statistical Models for the Plant and Soil Sciences* Ch. 1, 1–34 (CRC Press, Boca Raton, 2002).
25. Ingerson, T. E. & Buvel, R. L. Structure in asynchronous cellular automata. *Physica D* **10,** 59–68 (1984).

26. Matsuda, H., Ogita, N., Sasaki, A. & Sato, K. Statistical mechanics of population—the lattice Lotka–Volterra model. *Prog. Theor. Phys.* **88,** 1035–1049 (1992).
27. Kutznetsov, Y. A. & Levitin, V. V. *CONTENT: a Multiplatform Environment for Continuation and Bifurcation Analysis of Dynamical Systems* (Centrum voor Wiskunde en Informatica, Amsterdam, 1997).
28. Alados, C. L. *et al.* Change in plant spatial patterns and diversity along the successional gradient of Mediterranean grazing ecosystems. *Ecol. Modell.* **180,** 523–535 (2004).
29. Pueyo, Y. & Alados, C. L. Effects of fragmentation, abiotic factors and land use on vegetation recovery in a semi-arid Mediterranean area. *Basic Appl. Ecol.* **8,** 158–170 (2007).
30. Pascual, M., Roy, M., Guichard, F. & Flierl, G. Cluster size distributions: signatures of self-organization in spatial ecologies. *Phil. Trans. R. Soc. Lond. B* **357,** 657–666 (2002).

Acknowledgements The data collection was part of the DRASME (Desertification Risk Assessment in Silvopastoral Mediterranean Ecosystems) Collaborative Research Project. DRASME is funded by the EU under the INCO-DC Program. We acknowledge the assistance of M. Vrachnakis, D. Sirkou and K. Iovi in collecting the field data in Greece. The research of S.K. and M.R. is supported by a personal VIDI grant from the Netherlands Organization of Scientific Research/Earth and Life Sciences (NWO-ALW) to M.R. The research of Y.P. is funded by the Secretaría de Estado de Universidades e Investigación of Ministerio de Educación y Ciencia (Spain). The research of P.C.d.R. is supported by the LNV-NL Strategic Research Program ''Sustainable spatial development of ecosystems, landscapes and regions''. We are grateful to M. Kéfi for his help with the figures, and to R. C. G. Chaves for commenting on the manuscript.

Author Contributions The data collection was organized and carried out by C.L.A. (Spanish, Greek and Moroccan sites), V.P.P. (Greek site) and A.E. (Moroccan site). Y.P. participated in the data collection in Spain. S.K. conducted the data analyses with help from C.L.A. and Y.P. S.K. performed the numerical simulations and analysis of the model in collaboration with M.R. and P.C.d.R., and wrote the manuscript. M.R. and P.C.d.R. supervised this work and were involved in the writing. All authors discussed the results and commented on the manuscript.

Author Information Reprints and permissions information is available at www.nature.com/reprints. The authors declare no competing financial interests. Correspondence and requests for materials should be addressed to S.K. (kefi@geo.uu.nl).

METHODS

Data collection. The data were collected in Spain, Greece and Morocco (Table 1). For each of these areas, the grazing history is well-known, and the grazing system is traditional. Three grazing pressures were identified in each area: low, medium and high. Animals (goats and sheep) were followed in the field. Their movement (located by Global Positioning System, GPS, and transferred to a map in a Geographic Information System) and the time spent in each site were recorded. Effective stocking rate was calculated as the average stocking rate multiplied by the percentage of time each grazing site was used[28]. Vegetation surveys were conducted in 2000 from April to June[28]. Transects were laid out, and the vegetation cover under the tape was recorded by measuring the starting and end points (in centimetres) of each species. We note that this is a one-dimensional measure, but the transect method is meant to give us an estimation of the patch sizes.

Data analysis. For each transect, the number and the sizes of the patches were calculated. If $P < 0.05$, the truncated power-law model was kept as the best model describing the data. For these statistical analyses, we removed the patch sizes that were only present once to minimize the effect of the transect sizes (those in Morocco were different from those in Greece and Spain). Being only present for a small fraction of the year, annuals were excluded from the analyses.

Model definition. At the cell level, our model is stochastic: each of the possible events that applies to a cell occurs with a probability per unit of time (that is, a rate). These rates can depend on the state of the four nearest neighbours. We call ρ_σ the fraction of $\{\sigma\}$-cells in the lattice (σ is $+$, 0 or $-$), and $q_{\sigma|\sigma'}$ the fraction of $\{\sigma\}$-cells in the neighbourhood of a $\{\sigma'\}$-cell. We express the colonization rate of a $\{0\}$-cell as: $w_{\{0,+\}} = \beta(\delta\rho_+ + (1-\delta)q_{+|0})G(\rho_+)$, where β represents the intrinsic seed production rate per vegetation cell multiplied by the survival and the germination probabilities; δ is the fraction of seeds dispersed all over the lattice ($1-\delta$ is the fraction dispersed in the nearest neighbourhood); G describes how seedling establishment depends on competition for resources. For simplicity, G is expressed as a linear function of ρ_+: $G(\rho_+) = \varepsilon - g\rho_+$, where ε is the establishment probability of seeds in a system without vegetation and g is the competitive effect of $\{+\}$-cells on the establishment of new individuals. Let b be $\beta\varepsilon$. We assume that mortality is density-independent: $w_{\{+,0\}} = m$. Degradation of the soil of a $\{0\}$-cell occurs at a density-independent rate: $w_{\{0,-\}} = d$. Seeds cannot germinate on $\{-\}$-cells. Regeneration of a $\{-\}$-cell occurs at rate $w_{\{-,0\}} = r + fq_{+|-}$, with r the regeneration rate of a $\{-\}$-cell without vegetation in its neighbourhood. Local facilitation f is the positive effect of neighbouring $\{+\}$-cells on regeneration. A higher local facilitation means that, for a given number of $\{+\}$-cells in the neighbourhood of a $\{-\}$-cell, the regeneration of the $\{-\}$-cell is faster.

Model analysis. Once the densities reached a stationary state, the number and size of the vegetation patches were calculated at each time step during 2,000 time steps. Patch-size distributions were obtained by averaging the values of these 2,000 time steps[30]. The size of a patch is the number of cells that constitutes it. Patch-size distributions have a different range of ordinate values in the model and in the data. In the model, we indeed averaged the distributions over 2,000 time steps, whereas in the data we only have one distribution per site. We modelled grazing pressure as a higher mortality of $\{+\}$-cells. We used the correlation approximation[26] to analyse our model[3]. This method allowed the numerical derivation of bifurcation diagrams with the software CONTENT[3,27].

Parameter values used for the simulations. In the top row of Fig. 2 (local interactions decreasing from left to right): $m = 0.15$, $b = 0.8$, $d = 0.2$, $c = 0.3$, $r = 0.0001$. In Fig. 2a, $f = 0.52$, $\delta = 0.58$. In Fig. 2b, $f = 0.45$, $\delta = 0.65$. In Fig. 2c, $f = 0.4$, $\delta = 0.7$. A qualitatively similar result is obtained if f is varied and δ remains constant. In the bottom row of Fig. 2 (grazing pressure increasing from left to right): $\delta = 0.1$, $b = 0.6$, $f = 0.9$, $d = 0.2$, $c = 0.3$, $r = 0.0001$. In Fig. 2d, $m = 0.12$. In Fig. 2e, $m = 0.13$. In Fig. 2f, $m = 0.15$. A qualitatively similar result is obtained if aridity b is varied, with increasing aridity from left to right. In Fig. 3, $r = 0.9$, $\delta = 0.1$, $c = 0.3$, $d = 0.2$, $r = 0.0001$. In Fig. 3a, $m = 0.05$. In Fig. 3b, $m = 0.1$.